



# 1 **Interactions between aerosol organic components and liquid water content** 2 **during haze episodes in Beijing**

3 Xiaoxiao Li<sup>1</sup>, Shaojie Song<sup>2</sup>, Wei Zhou<sup>1</sup>, Jiming Hao<sup>1</sup>, Douglas R. Worsnop<sup>3,4</sup>, and Jingkun Jiang<sup>1\*</sup>

4 <sup>1</sup>State Key Joint Laboratory of Environment Simulation and Pollution Control, School of Environment, Tsinghua University,  
5 Beijing, 100084, China

6 <sup>2</sup>School of Engineering and Applied Sciences, Harvard University, Cambridge, Massachusetts 02138, USA

7 <sup>3</sup>Institute for Atmospheric and Earth System Research / Physics, Faculty of Science, University of Helsinki, Finland

8 <sup>4</sup>Aerodyne Research Inc., Billerica, Massachusetts 01821, USA

9 \*: Correspondence to: J. Jiang ([jiangjk@tsinghua.edu.cn](mailto:jiangjk@tsinghua.edu.cn))

10

11 **Abstract:** Aerosol liquid water (ALW) is ubiquitous in ambient aerosol and plays an important role in the formation of both  
12 aerosol organics and inorganics. To investigate the interactions between ALW and aerosol organics during haze formation and  
13 evolution, ALW was modelled based on long-term measurement of submicron aerosol composition in different seasons in  
14 Beijing. ALW contributed by aerosol inorganics ( $ALW_{inorg}$ ) was modelled by ISORROPIA-II, and ALW contributed by  
15 organics ( $ALW_{org}$ ) was estimated with  $\kappa$ -Köhler theory, where real-time hygroscopicity parameter of the organics ( $\kappa_{org}$ ) was  
16 calculated from the real-time organic oxygen-to-carbon (O/C). Overall particle hygroscopicity ( $\kappa_{total}$ ) was computed by  
17 weighting component hygroscopicity parameters based on their volume fractions in the mixture. We found that  $ALW_{org}$ , which  
18 is often neglected in traditional ALW modelling, contributes a significant fraction (18-32%) to the total ALW in Beijing. The  
19  $ALW_{org}$  fraction is largest in the cleanest days when both the organic fraction and  $\kappa_{org}$  are relatively high. The large variation  
20 of O/C, from 0.2 to 1.3, indicates the wide variety of organic components. This emphasizes the necessity of using real-time  
21  $\kappa_{org}$ , instead fixed  $\kappa_{org}$ , to calculate  $ALW_{org}$  in Beijing. The significant variation of  $\kappa_{org}$  (calculated from O/C), together with  
22 highly variable organic or inorganic volume fractions, leads to a wide range of  $\kappa_{total}$  (between 0.20 and 0.45), which has great  
23 impact on water uptake. The variation of organic O/C, or derived  $\kappa_{org}$ , was found to be influenced by T, ALW, and aerosol mass  
24 concentrations. Among which, T and ALW both have promoting effects on O/C. During high-ALW haze episodes, although  
25 the organic fraction decreases rapidly, O/C, and derived  $\kappa_{org}$ , increase with the increase in ALW, suggesting the formation of  
26 more soluble organics via aqueous/heterogeneous-phase process. A positive feedback loop is thus formed: during high-ALW  
27 episodes, increasing  $\kappa_{org}$ , together with decreasing particle organic fraction (or increasing particle inorganic fraction), increases  
28  $\kappa_{total}$ , thus further promotes the ability of particles to uptake water.

29

## 30 **1 INTRODUCTION**

31 Aerosol liquid water (ALW) is a ubiquitous component of ambient aerosol and exerts great influences on aerosol physical and  
32 chemical properties, especially in regions with high relative humidity (RH) (Cheng et al., 2016; Cheng et al., 2008; Covert et



33 al., 1972; Ervens et al., 2014; Nguyen et al., 2016; Pilinis et al., 1989; Zheng et al., 2015). From the perspective of aerosol  
34 physical processes, ALW influences particle lifetime, optical properties, radiative forcing, and the ability of particles to deposit  
35 in the humid human respiratory tract (Andreae and Rosenfeld, 2008; Cheng et al., 2008; Covert et al., 1972; Löndahl et al.,  
36 2008). ALW also promotes partitioning of some of the inorganic gases and water-soluble organic gases to the condensed phase,  
37 thus directly increasing aerosol mass loadings (Asa-Awuku et al., 2010; Parikh et al., 2011). From the perspective of aerosol  
38 chemical processes, ALW can serve as a reactor for heterogeneous/aqueous reactions, facilitating the formation of both  
39 secondary inorganics (Cheng et al., 2016; Sievering et al., 1991; Wang et al., 2016) and organics (Carlton et al., 2009; Ervens  
40 et al., 2014; Song et al., 2019). As a result, understanding ALW content is critical in clarifying the formation and evolution of  
41 ambient aerosols as well as their impacts on air quality and climate, especially in urban cities like Beijing where severe haze  
42 events take place frequently with elevated RH (Sun et al., 2013; Zheng et al., 2015).

43

44 The interaction between ALW and aerosol chemical composition is a key issue for haze formation but remains uncertain,  
45 especially regarding the interaction between ALW and aerosol organics. Studies have demonstrated that secondary inorganic  
46 aerosol (SIA) and secondary organic aerosol (SOA) surpass primary species during haze formation in China (Huang et al.,  
47 2014; Sun et al., 2016; Zheng et al., 2016). SOA or SIA-driven haze formation is widely observed to be associated with elevated  
48 relative humidity (RH), especially in winter. In Beijing, as RH rising from below 40% to above 60%, the following has been  
49 reported: (1) aerosol mass loadings increase significantly; (2) particles phase transition from solid/semisolid to liquid phase  
50 (Liu et al., 2017); (3) sulfur and nitrogen oxidation ratios both increase (Cheng et al., 2016; Sun et al., 2013; Zheng et al.,  
51 2015); (4) water-soluble inorganics increase faster than organics (Liu et al., 2015; Quan et al., 2015; Sun et al., 2013; Zheng  
52 et al., 2015). RH affects secondary species via heterogeneous/aqueous phase uptake or reactions. During haze episodes, gas  
53 phase photochemical formation of SIA and SOA is largely suppressed by the weakened solar radiation (Zheng et al., 2015).  
54 Formation of SIA and SOA is thus suggested to be dominated by heterogeneous/aqueous phase reactions (Xu et al., 2017),  
55 which are largely dependent on ALW. Based on ALW measurements, previous studies have proposed positive feedback loops  
56 in which elevated RH increases particle concentration and particle inorganic fraction; increased particle concentration and  
57 inorganic fraction in turn increase the water uptake (Cheng et al., 2016; Liu et al., 2017; Wu et al., 2018). However, whether  
58 or how elevated ALW affects the evolution of SOA during haze episodes remains less understood than that of SIA because of  
59 the complexity of SOA species.

60

61 Long-term data are needed to evaluate the amount of ALW and its interactions with aerosol organic compositions. So far,  
62 short-term ALW data in Beijing (Bian et al., 2014; Fajardo et al., 2016) have been collected by directly measuring size-resolved  
63 aerosol hygroscopic volume growth factors (VGF) and particle size distributions by hygroscopicity-tandem differential  
64 mobility analyzer (H-TDMA) (Rader and McMurry, 1986) or dry-ambient aerosol size spectrometer (DAASS) (Engelhart et



65 al., 2011; Stanier et al., 2004). However, long-term measurements of ALW are rare because of the challenge in sustaining these  
66 instruments. Another approach to obtain ALW is to combine aerosol chemical composition measurements and model  
67 predictions. ALW contributed by inorganics can be modelled by inorganic thermodynamic equilibrium models, such as  
68 ISORROPIA-II (Fountoukis and Nenes, 2007; Nenes et al., 1999, 1998), E-AIM (Clegg and Pitzer, 1992; Clegg et al., 1992),  
69 and SCAPE II (Kim et al., 1993a, b). Modelled inorganic water content is usually regarded as the total ALW because inorganic  
70 salts contribute a large fraction of the total particle loading and the hygroscopicity of inorganic salts is much larger (~6 times)  
71 than those of organic species (Bian et al., 2014; Hennigan et al., 2008). Although this approximation provides reasonable ALW  
72 in many ambient conditions, it fails in some cases. Especially when organics contribute a dominant fraction to particle loading,  
73 large discrepancies arise between the modelled inorganic water and the actual ALW content (Fajardo et al., 2016). Therefore,  
74 it is important to take the organic contribution to ALW into consideration. specific models include the calculation of organic  
75 ALW; e.g., aerosol diameter dependent equilibrium model (ADDEM) (Topping et al., 2005b, a). However, application of such  
76 models is hindered by lack of long-term measurements of specific OA species.

77

78 Recent studies have proposed a method to predict total ALW using the non-refractory submicron particulate matter (NR-PM<sub>1</sub>,  
79 particle diameter between 40 nm and 1 μm) composition measured with the widely used Aerosol Mass Spectrometer (AMS)  
80 (Nguyen et al., 2014; Nguyen et al., 2016). The inorganic contribution to ALW ( $ALW_{inorg}$ ) was modelled by ISORROPIA-II;  
81 organic contribution to ALW ( $ALW_{org}$ ) was estimated with  $\kappa$ -Köhler theory (Petters and Kreidenweis, 2007; Su et al., 2010).  
82 The total aerosol liquid water (ALW) is then the sum of  $ALW_{inorg}$  and  $ALW_{org}$ . ALW estimated by this method, which only  
83 requires aerosol chemical composition obtained from AMS measurements (Zhang et al., 2007), corresponds reasonably with  
84 measured ALW. Thus, this method can be used to predict long-term ALW from aerosol chemical composition and to explore  
85 interactions between ALW and organic evolution during haze events.

86

87 In this study, long-term NR-PM<sub>1</sub> chemical composition measurement was used to predict ALW in Beijing during various  
88 seasons (292 days in 5 years).  $ALW_{org}$  and  $ALW_{inorg}$  were estimated using  $\kappa$ -Köhler theory and ISORROPIA-II, respectively.  
89 A real-time organic hygroscopic parameter ( $\kappa_{org}$ , calculated from organic O/C ratio) was used to estimate  $ALW_{org}$ . The  
90 relationship between the total ALW and  $\kappa_{org}$  was explored. Within this long-term dataset, 12 high-ALW haze episodes and 8  
91 low-ALW haze episodes were identified. Chemical evolution during high-ALW and low-ALW haze episodes was found to  
92 differ significantly. Positive feedback between organic hygroscopicity, organic volume fraction, overall particle hygroscopicity,  
93 and ALW is proposed to be a factor driving severe haze formation in Beijing during high-ALW episodes



## 94 2 METHODOLOGY

### 95 2.1 Long-term measurements of particle chemical composition

96 Long-term field measurements were carried out between December 2013 and August 2017 at an urban site located on the  
97 campus of Tsinghua University in Beijing. The monitoring site is located on the top floor of a four-storey building without  
98 other tall buildings nearby with detailed information provided elsewhere (Cai and Jiang, 2017; Cao et al., 2014; He et al.,  
99 2001). Data from 292 days were used, including 2-3 months' data from each of the four seasons (Table S1). The average NR-  
100 PM<sub>1</sub> mass concentrations from spring to winter were 81.1, 54.2, 63.9, and 63.2 μg m<sup>-3</sup>, respectively. Note that PM<sub>2.5</sub>  
101 concentrations in Beijing were decreasing during this period (<http://www.bjepb.gov.cn/>).

102

103 Chemical composition of NR-PM<sub>1</sub>, including sulfate (SO<sub>4</sub><sup>2-</sup>), nitrate (NO<sub>3</sub><sup>-</sup>), ammonium (NH<sub>4</sub><sup>+</sup>), chloride (Cl<sup>-</sup>), and total  
104 organics (Org), was measured using a quadrupole aerosol chemical speciation mass spectrometer (Q-ACSM)(Ng et al., 2011).  
105 The Q-ACSM was calibrated before each measurement following the procedure described by Ng et al., (2011). The  
106 meteorological conditions, including temperature (*T*), relative humidity (RH), and other routine meteorological parameters,  
107 were recorded by a meteorological station.

### 108 2.2 Aerosol liquid water modelling

109 ALW<sub>inorg</sub> was modelled by ISORROPIA-II using meteorological conditions and the Q-ACSM measured inorganic  
110 compositions. The model was carried out with “reverse” and “metastable” mode. Compared to the “stable” mode, “metastable”  
111 mode assumes that particles are always aqueous droplets, even at low RH. Although some earlier studies observed phase  
112 transitions of ambient particles, recent studies suggest that ambient aerosols tend to be in “metastable” states due to the  
113 coexistence of organic compounds that inhibit or cover up the deliquescence and efflorescence behavior of inorganic  
114 compounds (Martin et al., 2008; Rood et al., 1989). The “metastable” mode predicts more water than predicted from “stable”  
115 mode when RH is between 40% and 70%, while similar with the latter when RH is above 70% or below 40% (Fig. S1),  
116 consistent with previous work (Song et al., 2018). In a few of the modelling results in summer and autumn, high acid/base  
117 ratio caused some of the NO<sub>3</sub><sup>-</sup> and Cl<sup>-</sup> to enter the gas phase in the form of HNO<sub>3</sub> and HCl, resulting in disagreement between  
118 the output liquid phase NO<sub>3</sub><sup>-</sup> and Cl<sup>-</sup> and the input aerosol phase NO<sub>3</sub><sup>-</sup> and Cl<sup>-</sup>. These points were removed.

119

120 ALW<sub>org</sub> was estimated using a simplified equation of κ-Köhler theory where Kelvin effect was neglected (Petters and  
121 Kreidenweis, 2007) (Eq. 1),

$$122 \quad ALW_{org} = V_{org} \kappa_{org} \frac{a_w}{1-a_w} \quad (1)$$



123 where  $a_w$  is the water activity and was assumed to be the same as RH (Bassett and Seinfeld, 1983) and  $V_{org}$  is the volume  
124 concentration of organics measured by Q-ACSM (density of organics was assumed to be  $1.2 \text{ g cm}^{-3}$ ). In previous studies, a  
125 fixed  $\kappa_{org}$  in the range of 0.06-0.13 was used for urban, urban downwind, and rural sites (Gunthe et al., 2011; Nguyen et al.,  
126 2016; Rose et al., 2011). However, the hygroscopicity of organics is highly variable and  $\kappa_{org}$  can vary between 0 and 0.3 for  
127 different species (Lambe et al., 2011; Massoli et al., 2010).  $\kappa_{org}$  was found to have a positive linear relationship with organic  
128 O/C ratio (Chang et al., 2010; Dick et al., 2000; Duplissy et al., 2011; Gunthe et al., 2011; Petters et al., 2009), which likely  
129 reflects combined effects of molecular weight, volatility, and surface activity (Nakao, 2017; Wang et al., 2019). Previous  
130 studies proposed several empirical methods to calculate  $\kappa_{org}$  from O/C derived from a series of chamber and field experiments  
131 (Chang et al., 2010; Duplissy et al., 2011; Jimenez et al., 2009; Lambe et al., 2011; Massoli et al., 2010). Comparing these  
132 methods (Table S2), Eq. 2 was used to calculate real-time  $\kappa_{org}$  over a broadest O/C range (0.05-1.42) (Lambe et al., 2011),

$$\kappa_{org} = (0.18 \pm 0.04) \times O/C + 0.03 \quad (2)$$

134 where real-time O/C was calculated from Q-ACSM measured  $f_{44}$  (the fraction of  $m/z$  44 fragments signal to total organic signal,  
135  $O/C = 0.079 + 4.31 \times f_{44}$ ) which has been widely used to study the aging process of OA species (Canagaratna et al., 2015; Ng  
136 et al., 2010).

137  
138 The Zdanovskii-Stokes-Robinson (ZSR) mixing rule was used to calculate the total ALW. According to ZSR, the total water  
139 uptake into internally mixed particles is the sum of water content uptake by each pure component (Jing et al., 2018).

140  
141 Particle hygroscopic volume growth factor (VGF) is the ratio of the volume of the wet particle to the corresponding particle  
142 volume at dry conditions. The size-independent VGF was calculated using Eq. 3,

$$\text{VGF} = \frac{\sum \frac{m_{i,ACSM}}{\rho_i} + (ALW_{inorg} + ALW_{org})/\rho_{water}}{\sum \frac{m_{i,ACSM}}{\rho_i}} \quad (3)$$

144 where  $m_{i,ACSM}$  is the mass concentration of species “i” measured by Q-ACSM. The densities were assumed to be 1.75, 1.75,  
145 1.75, 1.52, 1.2, and  $1.0 \text{ g cm}^{-3}$  for sulfate, nitrate, ammonium, chloride, organics, and water, respectively (Salcedo et al., 2006).

146  
147 Overall particle hygroscopicity ( $\kappa_{total}$ ) was computed by weighting component hygroscopicity parameters by their volume  
148 fractions in the mixture (Dusek et al., 2010; Gunthe et al., 2009; Petters and Kreidenweis, 2007) (Eq. 4),

$$\kappa_{total} = \kappa_{inorg} \cdot \text{frac}_{inorg} + \kappa_{org} \cdot \text{frac}_{org} \quad (4)$$

150 where  $\text{frac}_{inorg}$  and  $\text{frac}_{org}$  are the inorganic and organic volume fractions in NR-PM<sub>1</sub>, respectively. Inorganic species are mainly  
151 in the form of  $\text{NH}_4\text{NO}_3$ ,  $\text{H}_2\text{SO}_4$ ,  $\text{NH}_4\text{HSO}_4$ , and  $(\text{NH}_4)_2\text{SO}_4$  (Liu et al., 2014); corresponding hygroscopic parameters were  
152 0.68, 0.68, 0.56, and 0.52, respectively. As a result, an average value of 0.6 was used as the hygroscopicity parameter of the  
153 inorganic components ( $\kappa_{inorg}$ ), with the assumption that the relative abundance of  $\text{NH}_4\text{NO}_3$ ,  $\text{H}_2\text{SO}_4$ ,  $\text{NH}_4\text{HSO}_4$ , and  $(\text{NH}_4)_2\text{SO}_4$



154 does not change significantly. Thus in our study, variation of  $\kappa_{total}$  with RH only reflects changes in  $frac_{org}$  and  $\kappa_{org}$ .

## 155 **2.3 Haze episode identification**

156 The haze pollution in Beijing have shown typical evolution pattern where a pollution episode usually starts with a clean day,  
157 then accumulates for 2-7 days, and eventually disappears within 1-2 days (Guo et al., 2014; Zheng et al., 2016). In this study,  
158 22 haze episodes were identified (Table S3). Only episodes containing 4 or more than 4 calendar days were taken into  
159 consideration. The haze episodes were further classified according to ALW volume fraction; that is, the ratio of ALW volume  
160 to the wet particle total volume ( $ALW \text{ volume fraction} = V_{ALW} / (V_{ALW} + V_{NR-PM1})$ ). 12 were distinguished as high-ALW haze  
161 episodes ( $ALW \text{ volume fraction} > 0.3$  for at least 50% of the haze period), while 8 were distinguished as low-ALW haze  
162 episodes. All 20 distinguished episodes were associated with growing RH, the other 2 two with irregular RH variations were  
163 classified as undefined. Average NR-PM<sub>1</sub> mass concentrations for the high-ALW and low-ALW episodes were  $100.8 \mu\text{g m}^{-3}$   
164 and  $76.2 \mu\text{g m}^{-3}$ , respectively.

165

166 The relative daily increments of  $frac_{org}$ ,  $\kappa_{org}$ ,  $\kappa_{org} \cdot frac_{org}$  (indicates the contribution of organics to  $\kappa_{total}$ ), and  $\kappa_{total}$  during the  
167 classified 12 high-ALW haze episodes and 8 low-ALW haze episodes were averaged separately. Daily increments were used,  
168 not hourly increments, to avoid the impact of diurnal variability. The first and last day of the episodes were not included in the  
169 analysis as they were usually clean days, so that the chemical evolution was different from the hazy days. To minimize the  
170 influence of transport or large local primary emissions, the relative daily increments of more than 40% were not included in  
171 further analysis.

## 172 **3. RESULTS AND DISCUSSION**

### 173 **3.1 Aerosol liquid water contributed by organics**

174 The contribution of  $ALW_{org}$  to ALW is the highest when NR-PM<sub>1</sub> mass concentrations are below  $25 \mu\text{g m}^{-3}$ . In this low mass  
175 loading,  $ALW_{org}/ALW$  varies widely between ~10% and ~80%, with an average of 32% (Fig. 1a). The high  $ALW_{org}/ALW$  in  
176 low aerosol mass concentrations can be explained by high organics/NR-PM<sub>1</sub> mass fractions ( $57 \pm 15\%$ ) (as shown in Fig. 1b)  
177 and high  $\kappa_{org}$  (as shown in Fig. 2). The striking variability in  $ALW_{org}/ALW$  is the result of highly variable chemical  
178 compositions during clean days. In addition, higher uncertainties in NR-PM<sub>1</sub> measurements of low NR-PM<sub>1</sub> loadings and in  
179 ALW modelling at low RH may also contribute to the large variability. High  $ALW_{org}/ALW$  in low aerosol mass concentrations  
180 is consistent with previous studies (Dick et al., 2000; Fajardo et al., 2016). Those studies showed that modelled  $ALW_{inorg}$  was  
181 much lower than measured total ALW under low aerosol mass loadings in Beijing (Fajardo et al., 2016) and that  $ALW_{org}$  was



182 comparable to  $ALW_{inorg}$  in low RH (Dick et al., 2000).

183

184 As NR-PM<sub>1</sub> mass concentrations below 25  $\mu\text{g m}^{-3}$  increase to above 100  $\mu\text{g m}^{-3}$ ,  $ALW_{org}/ALW$  fraction decreases from an  
185 average of 32% to 18% in Beijing (Fig. 1a). This decrease is mainly caused by the decrease of organics/NR-PM<sub>1</sub> mass fractions  
186 from an average of 57% to 34% (Fig. 1b), and the decrease in organic/NR-PM<sub>1</sub> correlates with elevated RH, as indicated by  
187 the color of the scattered points. Although organic concentration increases with rising RH and NR-PM<sub>1</sub>, the concentration of  
188 inorganic water-soluble salts increases even more, leading to a decreased fraction of organics. Variation of  $ALW_{org}/ALW$   
189 narrows as NR-PM<sub>1</sub> mass concentration increase. During high aerosol concentration, the aerosols are aged and dominated by  
190 secondary species (Huang et al., 2014); while during low concentration, the origins of aerosol are more complex and variable.  
191 As a result, the chemical composition of NR-PM<sub>1</sub> become more homogeneous with the increase in NR-PM<sub>1</sub>.

192

193  $ALW_{org}$  calculated using the real-time  $\kappa_{org}$  is much larger than that using a fixed  $\kappa_{org}$  (0.08), which has often been used to  
194 represent the hygroscopicity of urban organic aerosols (Nguyen et al., 2016). However,  $\kappa_{org}$  in Beijing varies remarkably  
195 between 0.06 and 0.26, with an average of  $0.16 \pm 0.04$ , much higher than 0.08. This higher  $\kappa_{org}$  results in a higher  $ALW_{org}$   
196 fraction (18-32%) calculated in our study than predicted in previous ones (Nguyen et al., 2016; Wu et al., 2018). We note  
197 higher  $\kappa_{org}$  could be introduced via the conversion from organic O/C (Eq. 2); though  $\kappa_{org}$  calculated from others  
198 parameterizations (Chang et al., 2010; Duplissy et al., 2011; Peter et al., 2006; Raatikainen et al., 2010) are even higher than  
199 from the one used here (Fig. S2). Also, based on previous reports that Q-ACSM can report higher  $f_{44}$  values than the HR-ToF-  
200 AMS (Fröhlich et al., 2015), there is a possibility that positive deviations of  $f_{44}$  were introduced via the Q-ACSM measurements.  
201 Despite these possibilities, the large variations in  $\kappa_{org}$  emphasize the need to use real-time  $\kappa_{org}$  instead of a fixed value. When  
202 real-time  $\kappa_{org}$  is not available, at least a localized average  $\kappa_{org}$  should be considered.

### 203 **3.2 Influence of temperature, ALW, and NR-PM<sub>1</sub> mass concentrations on organic hygroscopicity**

204 Organic O/C ratio, and the derived organic hygroscopicity, increase with temperature ( $T$ ) for all the four seasons (Fig. 2). This  
205 positive correlation is more significant when  $T$  is below 15 °C. For the different seasons, average O/C ratios for summer, spring,  
206 autumn, and winter are 0.96, 0.82, 0.70, and 0.55, with corresponding average  $T$  of 27.6, 14.6, 10.0, and 2.3 °C, respectively.  
207 Diurnally, organic O/C show clear peaks at 14:00-16:00 which matches the diurnal variation of  $T$  well (Fig. S3). Similar diurnal  
208 changes of organic O/C have been previously observed (Hu et al., 2016; Sun et al., 2016). The promoting effect of  $T$  upon O/C  
209 can be attributed to multiple processes. On one hand,  $T$  often correlates with higher solar radiation and atmospheric oxidative  
210 capacity. On the other hand, higher  $T$  accelerates gas phase and aqueous/heterogeneous phase reactions and thus increases O/C.  
211 In addition, higher  $T$  promotes the partitioning of semi-volatile species from particle phase to gas phase, also resulting in an  
212 increase in O/C.



213

214 Fig. 3 shows the influence of ALW and NR-PM<sub>1</sub> mass concentration on organic O/C, or organic hygroscopicity. The cross-  
215 impact of *T* to O/C was separated by looking at the same color in Fig. 3. When ALW volume fraction is high (above 0.2-0.3),  
216 organic O/C tends to increase with increasing ALW volume fraction; the increasing trend was most significant for spring and  
217 autumn, while less significant for winter (Fig. 3a, c, d). The area between the two black lines in Fig. 3a, c, d is dominated by  
218 the influence of ALW. Elevated ALW facilitates aqueous/heterogeneous reactions and promotes the formation of more oxidized  
219 organics, such as dicarboxylic acids, thus increases O/C.

220

221 When ALW volume fraction is low (below 0.2-0.3), organic O/C decreases with lower NR-PM<sub>1</sub> mass concentration, indicated  
222 by the size of the scattered points; this was observed in spring, autumn, and winter. One reason might be that at extremely low  
223 aerosol mass concentrations, new particle formation events frequently occur and smaller particles dominate size distribution  
224 (Cai et al., 2017; Guo et al., 2014). During formation and initial growth of new particles, extremely low volatile organic  
225 compounds with the highest O/C ratio dominate; while subsequent growth involves organics with higher volatility and lower  
226 O/C ratio (Donahue et al., 2013; Ehn et al., 2014). As a result, particle organic O/C decreases with growth of aerosol mass  
227 concentration during new particle formation and growth events. Another possibility is that increased aerosol mass often  
228 coincides with diminished solar radiation which suppresses photochemistry and may decrease organic O/C. In addition, a  
229 fraction of the particles during clean periods are transported from less populated mountain areas. During such long-range  
230 transport, atmospheric oxidation can increase O/C. Low ALW volume fraction correlates with low NR-PM<sub>1</sub> mass loadings,  
231 which makes it look like organic O/C is decreasing with increasing ALW volume fraction. Overall, the apparent opposite trends  
232 during high and low ALW volume fraction periods can actually be explained by a competition between the opposite impact of  
233 ALW and NR-PM<sub>1</sub> mass loadings on organic evolution. However, summer was an exception, where no obvious dependence  
234 of organic O/C on ALW volume fraction or NR-PM<sub>1</sub> mass concentration was observed.

235

236 The competing effects of ALW volume fractions and NR-PM<sub>1</sub> mass concentrations on organic O/C were further confirmed by  
237 comparing organic evolution during the high and low-ALW haze episodes. Fig. 4 shows two typical haze episodes in Beijing,  
238 with more chemical and meteorological information given in Fig. S5. During the high-ALW episode, where ALW contributes  
239 0.2 - 0.75 to the total aerosol volume, organic O/C increases with haze accumulation. The increase of nighttime O/C is more  
240 striking than that of daytime, likely due to the more abundant ALW at night (see Fig. S4). On the contrary, during the low-  
241 ALW episode, where ALW volume fraction does not exceed 30%, daytime organic O/C decreases despite the increasing ALW  
242 and *T*; this indicates that the decrease in O/C introduced by reduced photo-oxidation process and gas-particle partitioning is  
243 larger than the O/C increase from aqueous/heterogeneous reactions. Nighttime O/C remains relatively constant, suggesting  
244 that the promoting effect of aqueous/heterogeneous reactions on O/C is comparable to the reducing effects on O/C.



### 245 3.3 The influence of RH and particle hygroscopicity on particle hygroscopic volume growth factor

246 Particle volume growth factor increases rapidly with RH and particle hygroscopicity (Fig. 5). When RH is less than 80%,  
247 particle VGF increases slowly from 1 to 2.5 with rising RH; when RH exceeds 80%, VGF increases rapidly to above 5. This  
248 is generally consistent with previous studies (Bian et al., 2014). As shown in Fig. 5, significant variation of  $\kappa_{total}$  also plays an  
249 important role in the change of water uptake. The dispersion of points in the vertical direction represents the influence of  
250 particle chemical compositions to ALW. For instance, when RH is fixed at 60%, VGF increases from 1.2 to 1.9 when  $\kappa_{total}$   
251 increases from ~0.20 to ~0.45.

252

253 The seasonal variations also reflect a combined promoting effect of RH and  $\kappa_{total}$  on VGF. The average VGFs for spring,  
254 summer, autumn, and winter are 1.4, 1.6, 1.3, and 1.3, respectively. The highest VGF in summer is attributed to a combination  
255 of the higher frequency for high RH (red step line, compared to green, orange, and blue step line in Fig. 5b) and the relatively  
256 high particle hygroscopicity,  $\kappa_{total}$  (0.35, compared to 0.38, 0.30, and 0.33 for other seasons).

257

258 A consequence of the high RH and high ALW is the higher particle overall hygroscopicity,  $\kappa_{total}$ , as compared with that at the  
259 low RH (Fig. 5). Aerosols are dominated by less hygroscopic particles ( $\kappa_{total} < 0.3$ ) for RH below ~40% while aerosols are  
260 dominated by more hygroscopic particles ( $\kappa_{total} > 0.4$ ) for RH above ~80% (Fig. 5). This suggests positive feedback between  
261 overall particle hygroscopicity and ALW. Higher  $\kappa_{total}$  leads to higher ALW in similar RH while higher ALW, or higher RH, in  
262 turn corresponds to higher  $\kappa_{total}$ .

### 263 3.4 Interactions between organic evolution and particle hygroscopicity during high and low-haze 264 episodes

265 During high-ALW episodes, the organic volume fraction decreases and organic hygroscopicity increases substantially during  
266 the accumulation of pollution. The average  $frac_{org}$  is 0.51 and the daily increment of  $frac_{org}$  is -11% (Fig. 6). The negative  
267  $frac_{org}$  increment indicates decreasing  $frac_{org}$  which reflects the larger increase of inorganic soluble compounds (sulfate, nitrate,  
268 ammonium, and chloride) compared to that of organics during haze episodes. The average  $\kappa_{org}$  is 0.165 and the relative daily  
269 increment of  $\kappa_{org}$  is 8%. The positive  $\kappa_{org}$  increment during high-ALW episodes reflects increasing  $\kappa_{org}$  due to the effect of  
270 aqueous/heterogeneous reactions. To sum up, although the organic fraction decreases during the high-ALW haze episodes, the  
271 organic hygroscopicity increases. As a result, the contribution of  $ALW_{org}$  to total ALW does not decrease as fast as the decrease  
272 of organic fraction.

273

274 During low-ALW episodes, the decrease in organic volume fraction is slower than that during high-ALW episodes, and organic



275 hygroscopicity hardly changes in the haze evolution process. The average  $frac_{org}$  is 0.63 and the daily increment of  $frac_{org}$  is -  
276 4% (Fig. 6), of which both are higher than those in high-ALW episodes. This suggests that organic is still the dominating  
277 component as haze accumulated during low-ALW episodes. The average  $\kappa_{org}$  is 0.152 and the relative daily increment of  $\kappa_{org}$  is  
278 -1%, both of which are lower than those in high-ALW episodes. The near zero increment of  $\kappa_{org}$  is a consequence of the  
279 competition between aqueous/heterogeneous reactions and other processes. To sum up, the effects of ALW on chemical  
280 compositions during low-ALW episodes are limited compared to high-ALW episodes.

281

282 As a consequence of the more significant changes in chemical composition during high-ALW episodes, the increase in particle  
283 hygroscopicity is larger for high-ALW episodes than for low-ALW episodes. The relative daily increments of  $frac_{org} \cdot \kappa_{org}$  during  
284 high-ALW and low-ALW episodes are -4% and -3%, respectively (Fig. 6c). These negative increments indicate the negative  
285 effect of the organic hygroscopic term on  $\kappa_{total}$  during haze episodes. For high-ALW episodes, this means that the increase in  
286 organic hygroscopicity in high-ALW episodes does not compensate for the effect of decreasing organic fraction. However, the  
287 average daily increments of  $\kappa_{total}$  during high-ALW and low-ALW haze episode are 8% and 2%, respectively (Fig. 6d). As  $\kappa_{inorg}$   
288 is fixed to 0.6 and the increment of  $frac_{inorg}$  is opposite to that of  $frac_{org}$ , the positive  $\kappa_{total}$  increment is a result of the positive  
289 increment of the term  $frac_{inorg} \cdot \kappa_{inorg}$ .

290

291 The rapid decrease in  $frac_{org}$  and increase in  $\kappa_{org}$  during high-ALW episodes increase  $\kappa_{total}$ , which in turn promotes the ability  
292 of particles to uptake water, forming positive feedbacks with ALW. The decrease of  $frac_{org}$  or increase of  $frac_{inorg}$  plays a  
293 dominating role while the increase in  $\kappa_{org}$  plays a minor but non-negligible role in increasing  $\kappa_{total}$ . During low-ALW episodes,  
294 the positive feedbacks are weak or does not exist because both  $frac_{org}$  and  $\kappa_{org}$  do not change significantly.

295

296 There are other factors, not taken into consideration here, that might also affect ALW. These factors include the presence of  
297 crustal material or trace metals, detailed particle size distributions, interactions between inorganic and organic compounds,  
298 organic surfactants, and the particle phase state (Bian et al., 2014; Fountoukis and Nenes, 2007; Nakao, 2017; Ovadnevaite et  
299 al., 2017). As a result, we strongly encourage that long term measurements of ALW and  $\kappa_{org}$  be performed to test the results  
300 shown here or establish a more reliable relationship between organic properties and ALW in the real atmosphere.

## 301 4 Conclusion

302 Our study emphasizes the need to include aerosol liquid water contributed by organics ( $ALW_{org}$ ) in ALW modelling in Beijing,  
303 instead of only using the inorganic contribution to total ALW. The reason is that  $ALW_{org}$  contributes an average of 18-32% to  
304 the total ALW in Beijing, according to our modelling results with ISORROPIA-II,  $\kappa$ -Köhler theory, and the ZSR mixing rule.



305 It is also necessary to use a real-time  $\kappa_{org}$  to evaluate  $ALW_{org}$ , since organic O/C, which has been shown in previous studies to  
306 have a linear relationship with  $\kappa_{org}$ , varies from 0.2 to 1.3 in different seasons in Beijing. Using a fixed  $\kappa_{org}$  (0.08) for typical  
307 urban areas underestimates  $ALW_{org}$  by a factor of  $\sim 2$  in Beijing. When real-time  $\kappa_{org}$  is not available, a localized average  $\kappa_{org}$   
308 should be used. O/C, or  $\kappa_{org}$ , generally increases with rising temperature and rising ALW in spring, autumn, and winter in  
309 Beijing.

310

311 Positive feedback loops were found between  $\kappa_{total}$  (which was determined by  $frac_{org}$  and  $\kappa_{org}$ , as  $\kappa_{inorg}$  was assumed to be 0.6)  
312 and ALW during high-ALW episodes, with a conceptual diagram shown in Fig. S6. During high-ALW haze episodes, the  
313 strong aqueous/heterogeneous phase reactions lead to a rapid decrease in  $frac_{org}$  and increase in  $\kappa_{org}$ . These variations increase  
314  $\kappa_{total}$ , thus further promoting the uptake of water and forming positive feedbacks. These positive feedbacks were much weaker  
315 in low-ALW episodes. The positive feedback loop between chemical composition evolution (mainly indicated by  $frac_{org}$  and  
316  $\kappa_{org}$ ) and ALW during high ALW-episodes is a driver for the severe haze episodes in Beijing.

## 317 Acknowledgments

318 Financial support from the National Key R&D Program of China (2016YFC0200102) and the National Science Foundation of  
319 China (91643201) is acknowledged.

## 320 Reference

- 321 Andreae, M. O., and Rosenfeld, D.: Aerosol-cloud-precipitation interactions. Part 1. The nature and sources of cloud-active  
322 aerosols, *Earth-Sci Rev*, 89, 13-41, 2008.
- 323 Asa-Awuku, A., Nenes, A., Gao, S., Flagan, R., and Seinfeld, J. H.: Water-soluble SOA from Alkene ozonolysis: composition  
324 and droplet activation kinetics inferences from analysis of CCN activity, *Atmos Chem Phys*, 10, 1585-1597, 2010.
- 325 Bassett, M., and Seinfeld, J. H.: ATMOSPHERIC EQUILIBRIUM-MODEL OF SULFATE AND NITRATE AEROSOLS,  
326 *Atmos Environ*, 17, 2237-2252, 10.1016/0004-6981(83)90221-4, 1983.
- 327 Bian, Y., Zhao, C., Ma, N., Chen, J., and Xu, W.: A study of aerosol liquid water content based on hygroscopicity measurements  
328 at high relative humidity in the North China Plain, *Atmos Chem Phys*, 14, 6417-6426, 2014.
- 329 Cai, R., and Jiang, J.: A new balance formula to estimate new particle formation rate: reevaluating the effect of coagulation  
330 scavenging, *Atmos Chem Phys*, 17, 12659-12675, 2017.
- 331 Cai, R., Yang, D., Fu, Y., Wang, X., Li, X., Ma, Y., Hao, J., Zheng, J., and Jiang, J.: Aerosol surface area concentration: a  
332 governing factor in new particle formation in Beijing, *Atmos Chem Phys*, 17, 12327, 2017.
- 333 Canagaratna, M. R., Jimenez, J. L., Kroll, J. H., Chen, Q., Kessler, S. H., Massoli, P., Hildebrandt Ruiz, L., Fortner, E., Williams,  
334 L. R., Wilson, K. R., Surratt, J. D., Donahue, N. M., Jayne, J. T., and Worsnop, D. R.: Elemental ratio measurements of organic  
335 compounds using aerosol mass spectrometry: characterization, improved calibration, and implications, *Atmos Chem Phys*, 15,  
336 253-272, 10.5194/acp-15-253-2015, 2015.
- 337 Cao, C., Jiang, W., Wang, B., Fang, J., Lang, J., Tian, G., Jiang, J., and Zhu, T. F.: Inhalable microorganisms in Beijing's PM<sub>2.5</sub>.



- 338 5 and PM10 pollutants during a severe smog event, *Environ Sci Technol*, 48, 1499-1507, 2014.
- 339 Carlton, A., Wiedinmyer, C., and Kroll, J.: A review of Secondary Organic Aerosol (SOA) formation from isoprene, *Atmos*  
340 *Chem Phys*, 9, 4987-5005, 2009.
- 341 Chang, R.-W., Slowik, J., Shantz, N., Vlasenko, A., Liggio, J., Sjostedt, S., Leitch, W., and Abbatt, J.: The hygroscopicity  
342 parameter ( $\kappa$ ) of ambient organic aerosol at a field site subject to biogenic and anthropogenic influences: relationship to degree  
343 of aerosol oxidation, *Atmos Chem Phys*, 10, 5047-5064, 2010.
- 344 Cheng, Y., Zheng, G., Wei, C., Mu, Q., Zheng, B., Wang, Z., Gao, M., Zhang, Q., He, K., Carmichael, G., Poschl, U., and Su,  
345 H.: Reactive nitrogen chemistry in aerosol water as a source of sulfate during haze events in China, *Science Advances*, 2,  
346 10.1126/sciadv.1601530, 2016.
- 347 Cheng, Y. F., Wiedensohler, A., Eichler, H., Heintzenberg, J., Tesche, M., Ansmann, A., Wendisch, M., Su, H., Althausen, D.,  
348 Herrmann, H., Gnauk, T., Brüeggemann, E., Hu, M., and Zhang, Y. H.: Relative humidity dependence of aerosol optical  
349 properties and direct radiative forcing in the surface boundary layer at Xinken in Pearl River Delta of China: An observation  
350 based numerical study, *Atmos Environ*, 42, 6373-6397, 10.1016/j.atmosenv.2008.04.009, 2008.
- 351 Clegg, S. L., and Pitzer, K. S.: Thermodynamics of multicomponent, miscible, ionic solutions: generalized equations for  
352 symmetrical electrolytes, *The Journal of Physical Chemistry*, 96, 3513-3520, 1992.
- 353 Clegg, S. L., Pitzer, K. S., and Brimblecombe, P.: Thermodynamics of multicomponent, miscible, ionic solutions. Mixtures  
354 including unsymmetrical electrolytes, *The Journal of Physical Chemistry*, 96, 9470-9479, 1992.
- 355 Covert, D. S., Charlson, R. J., and Ahlquist, N. C.: A study of the relationship of chemical composition and humidity to light  
356 scattering by aerosols, *Journal of Applied Meteorology*, 11, 968-976, 10.1175/1520-0450(1972)011<0968:asotro>2.0.co;2,  
357 1972.
- 358 Dick, W. D., Saxena, P., and McMurry, P. H.: Estimation of water uptake by organic compounds in submicron aerosols  
359 measured during the Southeastern Aerosol and Visibility Study, *Journal of Geophysical Research: Atmospheres*, 105, 1471-  
360 1479, 2000.
- 361 Donahue, N. M., Ortega, I. K., Chuang, W., Riipinen, I., Riccobono, F., Schobesberger, S., Dommen, J., Baltensperger, U.,  
362 Kulmala, M., Worsnop, D. R., and Vehkamäki, H.: How do organic vapors contribute to new-particle formation?, *Faraday*  
363 *discussions*, 165, 91-104, 10.1039/c3fd00046j, 2013.
- 364 Duplissy, J., DeCarlo, P. F., Dommen, J., Alfarra, M. R., Metzger, A., Barmapadimos, I., Prevot, A. S. H., Weingartner, E.,  
365 Tritscher, T., Gysel, M., Aiken, A. C., Jimenez, J. L., Canagaratna, M. R., Worsnop, D. R., Collins, D. R., Tomlinson, J., and  
366 Baltensperger, U.: Relating hygroscopicity and composition of organic aerosol particulate matter, *Atmos Chem Phys*, 11, 1155-  
367 1165, 10.5194/acp-11-1155-2011, 2011.
- 368 Dusek, U., Frank, G. P., Curtius, J., Drewnick, F., Schneider, J., Kuerten, A., Rose, D., Andreae, M. O., Borrmann, S., and  
369 Poeschl, U.: Enhanced organic mass fraction and decreased hygroscopicity of cloud condensation nuclei (CCN) during new  
370 particle formation events, *Geophys Res Lett*, 37, 10.1029/2009gl040930, 2010.
- 371 Ehn, M., Thornton, J. A., Kleist, E., Sipila, M., Junninen, H., Pullinen, I., Springer, M., Rubach, F., Tillmann, R., Lee, B.,  
372 Lopez-Hilfiker, F., Andres, S., Acir, I.-H., Rissanen, M., Jokinen, T., Schobesberger, S., Kangasluoma, J., Kontkanen, J.,  
373 Nieminen, T., Kurtén, T., Nielsen, L. B., Jorgensen, S., Kjaergaard, H. G., Canagaratna, M., Dal Maso, M., Berndt, T., Petaja,  
374 T., Wahner, A., Kerminen, V.-M., Kulmala, M., Worsnop, D. R., Wildt, J., and Mentel, T. F.: A large source of low-volatility  
375 secondary organic aerosol, *Nature*, 506, 476+, 10.1038/nature13032, 2014.
- 376 Engelhart, G. J., Hildebrandt, L., Kostenidou, E., Mihalopoulos, N., Donahue, N. M., and Pandis, S. N.: Water content of aged  
377 aerosol, *Atmos Chem Phys*, 11, 911-920, 10.5194/acp-11-911-2011, 2011.
- 378 Ervens, B., Sorooshian, A., Lim, Y. B., and Turpin, B. J.: Key parameters controlling OH-initiated formation of secondary  
379 organic aerosol in the aqueous phase (aqSOA), *J Geophys Res-Atmos*, 119, 3997-4016, 10.1002/2013jd021021, 2014.
- 380 Fajardo, O. A., Jiang, J., and Hao, J.: Continuous Measurement of Ambient Aerosol Liquid Water Content in Beijing, *Aerosol*  
381 *Air Qual Res*, 16, 1152-1164, 10.4209/aaqr.2015.10.0579, 2016.
- 382 Fountoukis, C., and Nenes, A.: ISORROPIA II: a computationally efficient thermodynamic equilibrium model for  $K^+-Ca^{2+}$ -  
383  $Mg^{2+}$ - $NH_4^+$ - $Na^+$ - $SO_4^{2-}$ - $NO_3^-$ - $Cl^-$ - $H_2O$  aerosols, *Atmos Chem Phys*, 7, 4639-4659, 2007.
- 384 Fröhlich, R., Crenn, V., Setyan, A., Belis, C. A., Canonaco, F., Favez, O., Riffault, V., Slowik, J. G., Aas, W., and Aijälä, M.:



- 385 ACTRIS ACSM intercomparison-Part 2: Intercomparison of ME-2 organic source apportionment results from 15 individual,  
386 co-located aerosol mass spectrometers, 2015.
- 387 Gunthe, S. S., King, S. M., Rose, D., Chen, Q., Roldin, P., Farmer, D. K., Jimenez, J. L., Artaxo, P., Andreae, M. O., Martin,  
388 S. T., and Poschl, U.: Cloud condensation nuclei in pristine tropical rainforest air of Amazonia: size-resolved measurements  
389 and modeling of atmospheric aerosol composition and CCN activity, *Atmos Chem Phys*, 9, 7551-7575, 2009.
- 390 Gunthe, S. S., Rose, D., Su, H., Garland, R. M., Achtert, P., Nowak, A., Wiedensohler, A., Kuwata, M., Takegawa, N., Kondo,  
391 Y., Hu, M., Shao, M., Zhu, T., Andreae, M. O., and Poschl, U.: Cloud condensation nuclei (CCN) from fresh and aged air  
392 pollution in the megacity region of Beijing, *Atmos Chem Phys*, 11, 11023-11039, 2011.
- 393 Guo, S., Hu, M., Zamora, M. L., Peng, J., Shang, D., Zheng, J., Du, Z., Wu, Z., Shao, M., and Zeng, L.: Elucidating severe  
394 urban haze formation in China, *Proceedings of the National Academy of Sciences*, 111, 17373-17378, 2014.
- 395 He, K., Yang, F., Ma, Y., Zhang, Q., Yao, X., Chan, C. K., Cadle, S., Chan, T., and Mulawa, P.: The characteristics of PM<sub>2.5</sub>  
396 in Beijing, China, *Atmos Environ*, 35, 4959-4970, 2001.
- 397 Hennigan, C. J., Bergin, M. H., Dibb, J. E., and Weber, R. J.: Enhanced secondary organic aerosol formation due to water  
398 uptake by fine particles, *Geophys Res Lett*, 35, 2008.
- 399 Hu, W., Hu, M., Hu, W., Jimenez, J. L., Yuan, B., Chen, W., Wang, M., Wu, Y., Chen, C., and Wang, Z.: Chemical composition,  
400 sources, and aging process of submicron aerosols in Beijing: Contrast between summer and winter, *Journal of Geophysical  
401 Research: Atmospheres*, 121, 1955-1977, 2016.
- 402 Huang, R.-J., Zhang, Y., Bozzetti, C., Ho, K.-F., Cao, J.-J., Han, Y., Daellenbach, K. R., Slowik, J. G., Platt, S. M., and  
403 Canonaco, F.: High secondary aerosol contribution to particulate pollution during haze events in China, *Nature*, 514, 218-222,  
404 2014.
- 405 Jimenez, J. L., Canagaratna, M. R., Donahue, N. M., Prevot, A. S. H., Zhang, Q., Kroll, J. H., DeCarlo, P. F., Allan, J. D., Coe,  
406 H., Ng, N. L., Aiken, A. C., Docherty, K. S., Ulbrich, I. M., Grieshop, A. P., Robinson, A. L., Duplissy, J., Smith, J. D., Wilson,  
407 K. R., Lanz, V. A., Hueglin, C., Sun, Y. L., Tian, J., Laaksonen, A., Raatikainen, T., Rautiainen, J., Vaattovaara, P., Ehn, M.,  
408 Kulmala, M., Tomlinson, J. M., Collins, D. R., Cubison, M. J., Dunlea, E. J., Huffman, J. A., Onasch, T. B., Alfarra, M. R.,  
409 Williams, P. I., Bower, K., Kondo, Y., Schneider, J., Drewnick, F., Borrmann, S., Weimer, S., Demerjian, K., Salcedo, D.,  
410 Cottrell, L., Griffin, R., Takami, A., Miyoshi, T., Hatakeyama, S., Shimono, A., Sun, J. Y., Zhang, Y. M., Dzepina, K., Kimmel,  
411 J. R., Sueper, D., Jayne, J. T., Herndon, S. C., Trimborn, A. M., Williams, L. R., Wood, E. C., Middlebrook, A. M., Kolb, C.  
412 E., Baltensperger, U., and Worsnop, D. R.: Evolution of Organic Aerosols in the Atmosphere, *Science*, 326, 1525-1529,  
413 10.1126/science.1180353, 2009.
- 414 Jing, B., Wang, Z., Tan, F., Guo, Y., Tong, S., Wang, W., Zhang, Y., and Ge, M.: Hygroscopic behavior of atmospheric aerosols  
415 containing nitrate salts and water-soluble organic acids, *Atmos Chem Phys*, 18, 5115-5127, 10.5194/acp-18-5115-2018, 2018.
- 416 Kim, Y. P., Seinfeld, J. H., and Saxena, P.: Atmospheric gas-aerosol equilibrium I. Thermodynamic model, *Aerosol Sci Tech*,  
417 19, 157-181, 1993a.
- 418 Kim, Y. P., Seinfeld, J. H., and Saxena, P.: Atmospheric gas-aerosol equilibrium II. Analysis of common approximations and  
419 activity coefficient calculation methods, *Aerosol Sci Tech*, 19, 182-198, 1993b.
- 420 Lambe, A. T., Onasch, T. B., Massoli, P., Croasdale, D. R., Wright, J. P., Ahern, A. T., Williams, L. R., Worsnop, D. R., Brune,  
421 W. H., and Davidovits, P.: Laboratory studies of the chemical composition and cloud condensation nuclei (CCN) activity of  
422 secondary organic aerosol (SOA) and oxidized primary organic aerosol (OPOA), *Atmos Chem Phys*, 11, 8913-8928,  
423 10.5194/acp-11-8913-2011, 2011.
- 424 Liu, H. J., Zhao, C. S., Nekat, B., Ma, N., Wiedensohler, A., van Pinxteren, D., Spindler, G., Mueller, K., and Herrmann, H.:  
425 Aerosol hygroscopicity derived from size-segregated chemical composition and its parameterization in the North China Plain,  
426 *Atmos Chem Phys*, 14, 2525-2539, 10.5194/acp-14-2525-2014, 2014.
- 427 Liu, X. G., Sun, K., Qu, Y., Hu, M., Sun, Y. L., Zhang, F., and Zhang, Y. H.: Secondary Formation of Sulfate and Nitrate during  
428 a Haze Episode in Megacity Beijing, China, *Aerosol Air Qual Res*, 15, 2246-2257, 10.4209/aaqr.2014.12.0321, 2015.
- 429 Liu, Y., Wu, Z., Wang, Y., Xiao, Y., Gu, F., Zheng, J., Tan, T., Shang, D., Wu, Y., Zeng, L., Hu, M., Bateman, A. P., and Martin,  
430 S. T.: Submicrometer Particles Are in the Liquid State during Heavy Haze Episodes in the Urban Atmosphere of Beijing,  
431 China, *Environ Sci Tech Lett*, 4, 427-432, 10.1021/acs.estlett.7b00352, 2017.



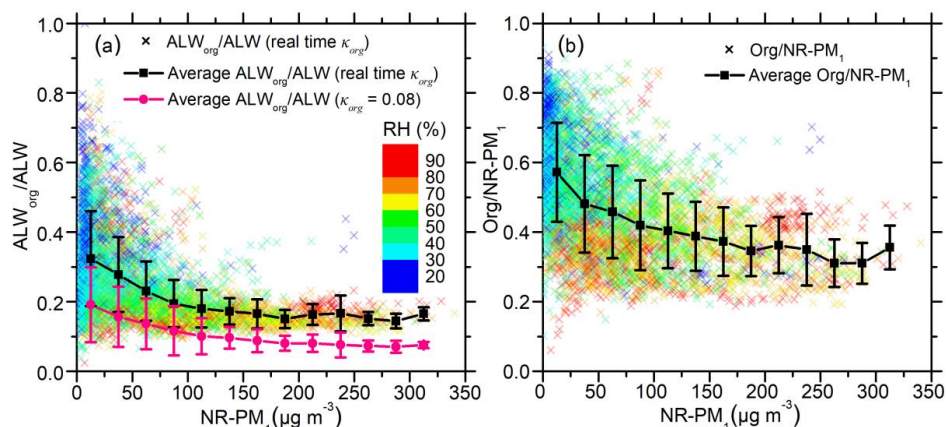
- 432 Löndahl, J., Pagels, J., Boman, C., Swietlicki, E., Massling, A., Rissler, J., Blomberg, A., Bohgard, M., and Sandström, T.:  
433 Deposition of biomass combustion aerosol particles in the human respiratory tract, *Inhalation toxicology*, 20, 923-933, 2008.
- 434 Martin, S. T., Rosenoern, T., Chen, Q., and Collins, D. R.: Phase changes of ambient particles in the Southern Great Plains of  
435 Oklahoma, *Geophys Res Lett*, 35, 2008.
- 436 Massoli, P., Lambe, A., Ahern, A., Williams, L., Ehn, M., Mikkilä, J., Canagaratna, M., Brune, W., Onasch, T., and Jayne, J.:  
437 Relationship between aerosol oxidation level and hygroscopic properties of laboratory generated secondary organic aerosol  
438 (SOA) particles, *Geophys Res Lett*, 37, 2010.
- 439 Nakao, S.: Why would apparent  $\kappa$  linearly change with O/C? Assessing the Role of Volatility, Solubility, and Surface Activity  
440 of Organic Aerosols, *Aerosol Sci Tech*, 1-12, 2017.
- 441 Nenes, A., Pandis, S. N., and Pilinis, C.: ISORROPIA: A new thermodynamic equilibrium model for multiphase  
442 multicomponent inorganic aerosols, *Aquatic geochemistry*, 4, 123-152, 1998.
- 443 Nenes, A., Pandis, S. N., and Pilinis, C.: Continued development and testing of a new thermodynamic aerosol module for  
444 urban and regional air quality models, *Atmos Environ*, 33, 1553-1560, 1999.
- 445 Ng, N. L., Canagaratna, M. R., Zhang, Q., Jimenez, J. L., Tian, J., Ulbrich, I. M., Kroll, J. H., Docherty, K. S., Chhabra, P. S.,  
446 Bahreini, R., Murphy, S. M., Seinfeld, J. H., Hildebrandt, L., Donahue, N. M., DeCarlo, P. F., Lanz, V. A., Prevot, A. S. H.,  
447 Dinar, E., Rudich, Y., and Worsnop, D. R.: Organic aerosol components observed in Northern Hemispheric datasets from  
448 Aerosol Mass Spectrometry, *Atmos Chem Phys*, 10, 4625-4641, 10.5194/acp-10-4625-2010, 2010.
- 449 Ng, N. L., Herndon, S. C., Trimborn, A., Canagaratna, M. R., Croteau, P. L., Onasch, T. B., Sueper, D., Worsnop, D. R., Zhang,  
450 Q., Sun, Y. L., and Jayne, J. T.: An Aerosol Chemical Speciation Monitor (ACSM) for Routine Monitoring of the Composition  
451 and Mass Concentrations of Ambient Aerosol, *Aerosol Sci Tech*, 45, 780-794, 2011.
- 452 Nguyen, T. K. V., Petters, M. D., Suda, S. R., Guo, H., Weber, R. J., and Carlton, A. G.: Trends in particle-phase liquid water  
453 during the Southern Oxidant and Aerosol Study, *Atmos Chem Phys*, 14, 10911-10930, 10.5194/acp-14-10911-2014, 2014.
- 454 Nguyen, T. K. V., Zhang, Q., Jimenez, J. L., Pike, M., and Carlton, A. G.: Liquid Water: Ubiquitous Contributor to Aerosol  
455 Mass, *Environ Sci Tech Lett*, 3, 257-263, 10.1021/acs.estlett.6b00167, 2016.
- 456 Ovadnevaite, J., Zuend, A., Laaksonen, A., Sanchez, K. J., Roberts, G., Ceburnis, D., Decesari, S., Rinaldi, M., Hodas, N., and  
457 Facchini, M. C.: Surface tension prevails over solute effect in organic-influenced cloud droplet activation, *Nature*, 546, 637,  
458 2017.
- 459 Parikh, H. M., Carlton, A. G., Vizuete, W., and Kamens, R. M.: Modeling secondary organic aerosol using a dynamic  
460 partitioning approach incorporating particle aqueous-phase chemistry, *Atmos Environ*, 45, 1126-1137, 2011.
- 461 Peter, T., Marcolli, C., Spichtinger, P., Corti, T., Baker, M. B., and Koop, T.: When dry air is too humid, *Science*, 314, 1399-  
462 1402, 2006.
- 463 Petters, M., Wex, H., Carrico, C., Hallbauer, E., Massling, A., McMeeking, G., Poulain, L., Wu, Z., Kreidenweis, S., and  
464 Stratmann, F.: Towards closing the gap between hygroscopic growth and activation for secondary organic aerosol—Part 2:  
465 Theoretical approaches, *Atmos Chem Phys*, 9, 3999-4009, 2009.
- 466 Petters, M. D., and Kreidenweis, S. M.: A single parameter representation of hygroscopic growth and cloud condensation  
467 nucleus activity, *Atmos Chem Phys*, 7, 1961-1971, 2007.
- 468 Pilinis, C., Seinfeld, J. H., and Grosjean, D.: WATER-CONTENT OF ATMOSPHERIC AEROSOLS, *Atmos Environ*, 23,  
469 1601-1606, 10.1016/0004-6981(89)90419-8, 1989.
- 470 Quan, J., Liu, Q., Li, X., Gao, Y., Jia, X., Sheng, J., and Liu, Y.: Effect of heterogeneous aqueous reactions on the secondary  
471 formation of inorganic aerosols during haze events, *Atmos Environ*, 122, 306-312, 10.1016/j.atmosenv.2015.09.068, 2015.
- 472 Raatikainen, T., Vaattovaara, P., Tiitta, P., Miettinen, P., Rautiainen, J., Ehn, M., Kulmala, M., Laaksonen, A., and Worsnop,  
473 D. R.: Physicochemical properties and origin of organic groups detected in boreal forest using an aerosol mass spectrometer,  
474 *Atmos Chem Phys*, 10, 2063-2077, 10.5194/acp-10-2063-2010, 2010.
- 475 Rader, D., and McMurry, P.: Application of the tandem differential mobility analyzer to studies of droplet growth or  
476 evaporation, *J Aerosol Sci*, 17, 771-787, 1986.
- 477 Rood, M., Shaw, M., Larson, T., and Covert, D.: Ubiquitous nature of ambient metastable aerosol, *Nature*, 337, 537-539, 1989.
- 478 Rose, D., Gunthe, S. S., Su, H., Garland, R. M., Yang, H., Berghof, M., Cheng, Y. F., Wehner, B., Achtert, P., Nowak, A.,



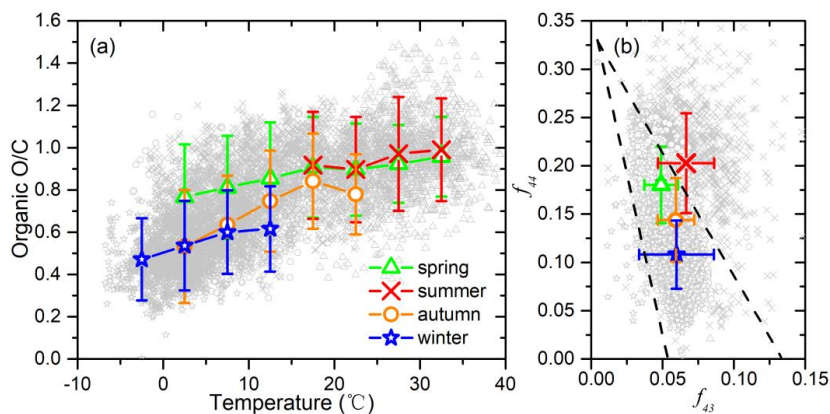
- 479 Wiedensohler, A., Takegawa, N., Kondo, Y., Hu, M., Zhang, Y., Andreae, M. O., and Poeschl, U.: Cloud condensation nuclei  
480 in polluted air and biomass burning smoke near the mega-city Guangzhou, China -Part 2: Size-resolved aerosol chemical  
481 composition, diurnal cycles, and externally mixed weakly CCN-active soot particles, *Atmos Chem Phys*, 11, 2817-2836,  
482 10.5194/acp-11-2817-2011, 2011.
- 483 Salcedo, D., Onasch, T. B., Dzepina, K., Canagaratna, M. R., Zhang, Q., Huffman, J. A., DeCarlo, P. F., Jayne, J. T., Mortimer,  
484 P., Worsnop, D. R., Kolb, C. E., Johnson, K. S., Zuberi, B., Marr, L. C., Volkamer, R., Molina, L. T., Molina, M. J., Cardenas,  
485 B., Bernabe, R. M., Marquez, C., Gaffney, J. S., Marley, N. A., Laskin, A., Shutthanandan, V., Xie, Y., Brune, W., Leshner, R.,  
486 Shirley, T., and Jimenez, J. L.: Characterization of ambient aerosols in Mexico City during the MCMA-2003 campaign with  
487 Aerosol Mass Spectrometry: results from the CENICA Supersite, *Atmos Chem Phys*, 6, 925-946, 2006.
- 488 Sievering, H., Boatman, J., Galloway, J., Keene, W., Kim, Y., Luria, M., and Ray, J.: Heterogeneous sulfur conversion in sea-  
489 salt aerosol particles: the role of aerosol water content and size distribution, *Atmospheric Environment. Part A. General Topics*,  
490 25, 1479-1487, 1991.
- 491 Song, S., Gao, M., Xu, W., Shao, J., Shi, G., Wang, S., Wang, Y., Sun, Y., and McElroy, M. B.: Fine-particle pH for Beijing  
492 winter haze as inferred from different thermodynamic equilibrium models, *Atmos Chem Phys*, 18, 7423-7438, 10.5194/acp-  
493 18-7423-2018, 2018.
- 494 Song, S., Gao, M., Xu, W., Sun, Y., Worsnop, D. R., Jayne, J. T., Zhang, Y., Zhu, L., Li, M., Zhou, Z., Cheng, C., Lv, Y., Wang,  
495 Y., Peng, W., Xu, X., Lin, N., Wang, Y., Wang, S., Munger, J. W., Jacob, D. J., and McElroy, M. B.: Possible heterogeneous  
496 chemistry of hydroxymethanesulfonate (HMS) in northern China winter haze, *Atmos Chem Phys*, 19, 1357-1371, 10.5194/acp-  
497 19-1357-2019, 2019.
- 498 Stanier, C. O., Khlystov, A. Y., Chan, W. R., Mandiro, M., and Pandis, S. N.: A Method for the In Situ Measurement of Fine  
499 Aerosol Water Content of Ambient Aerosols: The Dry-Ambient Aerosol Size Spectrometer (DAASS) Special Issue of Aerosol  
500 Science and Technology on Findings from the Fine Particulate Matter Supersites Program, *Aerosol Sci Tech*, 38, 215-228,  
501 2004.
- 502 Su, H., Rose, D., Cheng, Y. F., Gunthe, S. S., Massling, A., Stock, M., Wiedensohler, A., Andreae, M. O., and Poeschl, U.:  
503 Hygroscopicity distribution concept for measurement data analysis and modeling of aerosol particle mixing state with regard  
504 to hygroscopic growth and CCN activation, *Atmos Chem Phys*, 10, 7489-7503, 10.5194/acp-10-7489-2010, 2010.
- 505 Sun, Y., Du, W., Fu, P., Wang, Q., Li, J., Ge, X., Zhang, Q., Zhu, C., Ren, L., Xu, W., Zhao, J., Han, T., Worsnop, D. R., and  
506 Wang, Z.: Primary and secondary aerosols in Beijing in winter: sources, variations and processes, *Atmos. Chem. Phys.*, 16,  
507 8309-8329, 10.5194/acp-16-8309-2016, 2016.
- 508 Sun, Y. L., Wang, Z. F., Fu, P. Q., Jiang, Q., Yang, T., Li, J., and Ge, X. L.: The impact of relative humidity on aerosol  
509 composition and evolution processes during wintertime in Beijing, China, *Atmos Environ*, 77, 927-934,  
510 10.1016/j.atmosenv.2013.06.019, 2013.
- 511 Topping, D., McFiggans, G., and Coe, H.: A curved multi-component aerosol hygroscopicity model framework: Part 2–  
512 Including organic compounds, *Atmos Chem Phys*, 5, 1223-1242, 2005a.
- 513 Topping, D., McFiggans, G., and Coe, H.: A curved multi-component aerosol hygroscopicity model framework: Part 1–  
514 Inorganic compounds, *Atmos Chem Phys*, 5, 1205-1222, 2005b.
- 515 Wang, G., Zhang, R., Gomez, M. E., Yang, L., Zamora, M. L., Hu, M., Lin, Y., Peng, J., Guo, S., and Meng, J.: Persistent  
516 sulfate formation from London Fog to Chinese haze, *Proceedings of the National Academy of Sciences*, 113, 13630-13635,  
517 2016.
- 518 Wang, J., Shilling, J. E., Liu, J., Zelenyuk, A., Bell, D. M., Petters, M. D., Thalman, R., Mei, F., Zaveri, R. A., and Zheng, G.:  
519 Cloud droplet activation of secondary organic aerosol is mainly controlled by molecular weight, not water solubility, *Atmos.*  
520 *Chem. Phys.*, 19, 941-954, 10.5194/acp-19-941-2019, 2019.
- 521 Wu, Z., Wang, Y., Tan, T., Zhu, Y., Li, M., Shang, D., Wang, H., Lu, K., Guo, S., and Zeng, L.: Aerosol Liquid Water Driven  
522 by Anthropogenic Inorganic Salts: Implying Its Key Role in Haze Formation over the North China Plain, *Environ Sci Tech*  
523 *Let*, 5, 160-166, 2018.
- 524 Xu, W., Han, T., Du, W., Wang, Q., Chen, C., Zhao, J., Zhang, Y., Li, J., Fu, P., and Wang, Z.: Effects of Aqueous-Phase and  
525 Photochemical Processing on Secondary Organic Aerosol Formation and Evolution in Beijing, China, *Environ Sci Technol*,



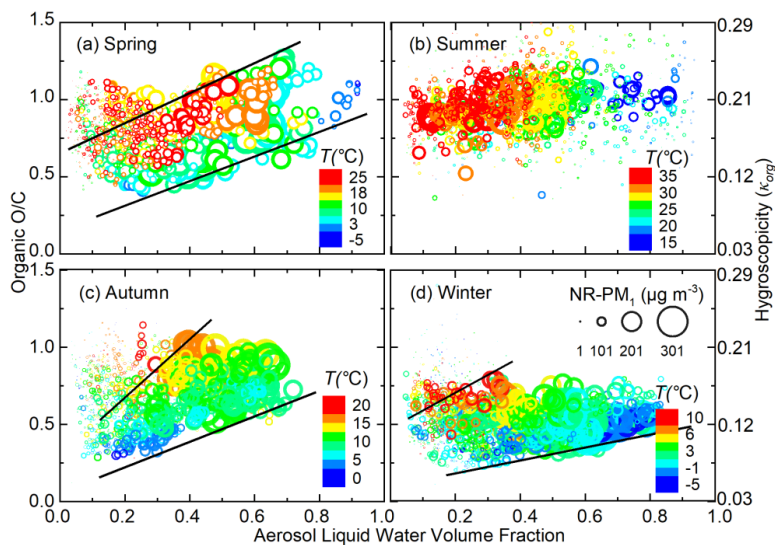
526 51, 762-770, 2017.  
527 Zhang, Q., Jimenez, J. L., Canagaratna, M. R., Allan, J. D., Coe, H., Ulbrich, I., Alfarra, M. R., Takami, A., Middlebrook, A.  
528 M., Sun, Y. L., Dzepina, K., Dunlea, E., Docherty, K., DeCarlo, P. F., Salcedo, D., Onasch, T., Jayne, J. T., Miyoshi, T.,  
529 Shimono, A., Hatakeyama, S., Takegawa, N., Kondo, Y., Schneider, J., Drewnick, F., Borrmann, S., Weimer, S., Demerjian,  
530 K., Williams, P., Bower, K., Bahreini, R., Cottrell, L., Griffin, R. J., Rautiainen, J., Sun, J. Y., Zhang, Y. M., and Worsnop, D.  
531 R.: Ubiquity and dominance of oxygenated species in organic aerosols in anthropogenically-influenced Northern Hemisphere  
532 midlatitudes, *Geophys Res Lett*, 34, 2007.  
533 Zheng, G., Duan, F., Ma, Y., Zhang, Q., Huang, T., Kimoto, T., Cheng, Y., Su, H., and He, K.: Episode-Based Evolution Pattern  
534 Analysis of Haze Pollution: Method Development and Results from Beijing, China, *Environ Sci Technol*, 50, 4632-4641,  
535 10.1021/acs.est.5b05593, 2016.  
536 Zheng, G. J., Duan, F. K., Su, H., Ma, Y. L., Cheng, Y., Zheng, B., Zhang, Q., Huang, T., Kimoto, T., Chang, D., Poeschl, U.,  
537 Cheng, Y. F., and He, K. B.: Exploring the severe winter haze in Beijing: the impact of synoptic weather, regional transport  
538 and heterogeneous reactions, *Atmos Chem Phys*, 15, 2969-2983, 10.5194/acp-15-2969-2015, 2015.  
539  
540



541  
 542 **Figure 1.** (a) The colored scatter points represent the fraction of aerosol liquid water contributed by organics ( $ALW_{org}/ALW$ ), which  
 543 was calculated using real-time  $\kappa_{org}$ . The black line shows the average of the colored points in each NR- $PM_{10}$  mass concentration bin.  
 544 The pink line is the average  $ALW_{org}/ALW$  calculated using a fixed  $\kappa_{org}$  (0.08) in each NR- $PM_{10}$  mass concentration bin. (b) The colored  
 545 scatter points represent the organic mass fraction in non-refractory submicron aerosol (NR- $PM_{10}$ ). The black line is the average of  
 546 the colored points in each NR- $PM_{10}$  mass concentration bin. All the scattered points in both figures are colored with relative humidity  
 547 (RH).  
 548



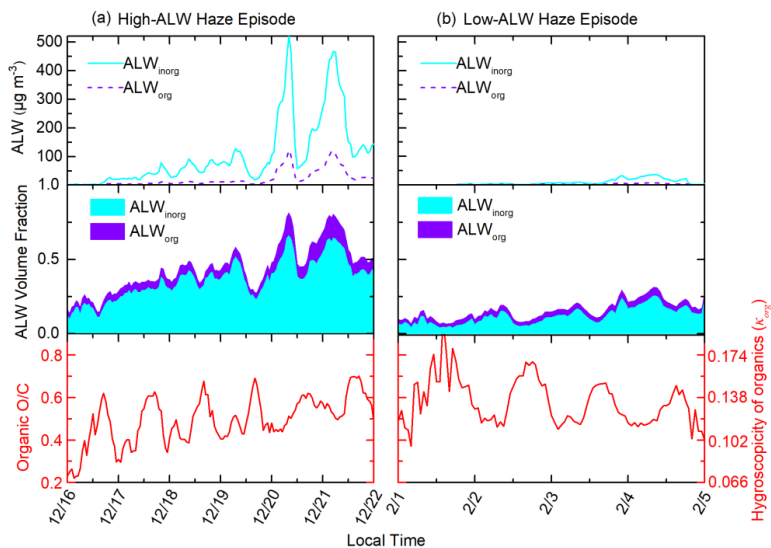
549  
 550 **Figure 2.** (a) O/C ratio as a function of temperature in different seasons; (b) triangle plot ( $f_{44}$  vs  $f_{43}$ ) measured by the Q-ACSM in  
 551 different seasons  
 552  
 553



554

555 **Figure 3.** Variation of organic O/C ratio (calculated from Q-ACSM measured  $f_{44}$ ) as a function of aerosol liquid water (ALW) volume  
 556 fraction in different seasons. The size and color of the points represent the corresponding NR-PM<sub>1</sub> mass concentration and ambient  
 557 temperature, respectively. For spring, autumn, and winter, the areas between the two black lines represent the points less affected  
 558 by the gas-particle partitioning under low aerosol mass loadings.

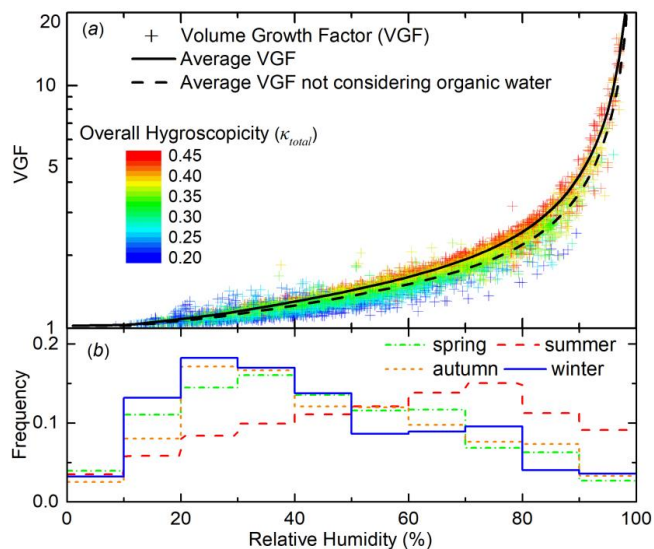
559



560

561 **Figure 4.** Variations of aerosol liquid water contributed by organics (ALW<sub>org</sub>), aerosol liquid water contributed by inorganics  
 562 (ALW<sub>inorg</sub>), the volume fraction of total wet particle compositions, organic O/C during (a) a typical high-ALW episode and (b) a  
 563 typical low-ALW episode.

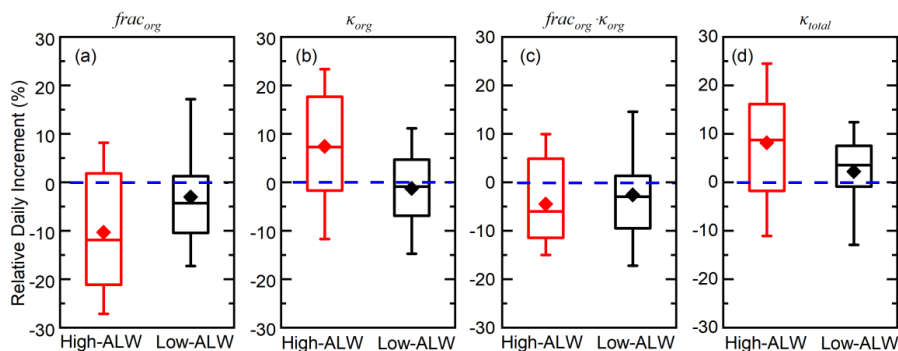
564



565

566 **Figure 5. (a) Volume growth factor (VGF, scattered points, calculated by Eq. 3) from the four seasons as a function of relative**  
 567 **humidity (RH). The points are colored by overall particle hygroscopicity ( $\kappa_{total}$ ) calculated from aerosol bulk composition (Eq. 4).**  
 568 **The black line is the averaged VGF in different RH. Black dashed line is the average VGF without considering organic water. (b)**  
 569 **RH frequency during four seasons is expressed in step line.**

570



571

572 **Figure 6. Episode-based relative day increment of organic hygroscopicity ( $\kappa_{org}$ ), organic volume fraction ( $frac_{org}$ ), the hygroscopicity**  
 573 **term contributed by organics ( $\kappa_{org} \cdot frac_{org}$ ), and overall particle hygroscopicity ( $\kappa_{total}$ ) during high-ALW haze episodes and low-ALW**  
 574 **haze episodes. The box plots represent the 10th, 25th, 50th, 75th, and 90th percentiles of the corresponding data. The rhombus**  
 575 **represents the mean value of the corresponding data.**

576